The comparison of characteristic and operating performance by pole-slot combinations in Interior Permanent Magnet Synchronous Motor with concentrated winding

Seung-Hyoung Ha*, Soon-O Kwon*, Ji-Hyung Bahn* and Jung-Pyo Hong*
* Chnagwon Nat'l., Univ., #9, Sarim-dong, Changwon, Gyeongnam, 641-773, Korea

***Abstract*-- The Interior Permanent Magnet Synchronous Motor (IPMSM) is widely used for several industrial applications, because the motor can have high performance due to the reluctance torque generated by the difference of d-q axes inductance, and then the motor has much more torque than the Surface Permanent Magnet Synchronous Motor (SPMSM).**

In order to miniature and improve the manufacture efficiency of the motor, it has concentrated winding, because concentrated winding can reduce the motor volume and make the manufacture be simpler compared with the distributed winding. When motor with concentrated winding is designed, pole-slot combinations are very important. In accordance with pole-slot combinations, the winding factor can be increased, and at the same time d-q axes inductance and saliency ratio are influenced. The parameters, such as back electromotive force (BEMF), d-q axes inductance, and saliency ratio, are very important which influent characteristics of the motor and operating performance. Therefore, this paper presents the comparison of characteristics and operating performance by pole-slot combinations in IPMSM with concentrated winding.

***Index Terms*—concentrated winding, interior permanent magnet synchronous motor, pole-slot combinations, winding factor.**

I. INTRODUCTION

Permanent magnet motors (PM motors) have a wide application because they offer excellent maintainability, controllability, and environmental endurance while providing high-efficiency operation at high power factor [1].

Interior Permanent Magnet Synchronous Motor (IPMSM) has high energy density, compared with Surface Permanent Magnet Synchronous Motor (SPMSM) because it has reluctance torque by difference of d-q axes inductance in addition to magnetic torque by the permanent magnet, and be easy using flux weakening control at constant power operation. Therefore IPMSM is increasingly employed for electric vehicles and compressor drives.

This work was supported by grant no.RTI04-01-03 from the regional technology innovation program of ministry of commerce, industry and energy (MOCIE).

The winding layouts of motor generally are divided into two layouts that are concentrated winding and distributed winding. The concentrated winding has shorter end winding and simpler structure suitable for high volume automated manufacturing in comparison with the distributed winding [2].

The motors with concentrated windings usually have low winding factors, and so have a low back electromotive force (BEMF). However winding factors can be increased in accordance with pole-slot combinations.

The winding factors also have influence upon d-q axes inductance. BEMF and d-q axes inductance which are important design parameters determine on constant torque region and constant power operation. Therefore winding factors in accordance with pole-slot combinations are very important factors.

The aim of this paper is to investigate design parameters and operating performance of IPMSM with different winding factors in accordance with pole-slot combinations.

II. WINDING FACTOR

IPMSM with concentrated windings usually has slot number of only 2/3 pole numbers, which results in a poor fundamental winding factor of 0.866. This can be compared to the ideal winding factor of one, which can easily be acquired using distributed windings [2]. However, by choosing better pole-slot combinations, the winding factor can be substantially increased.

Table I shows the results of winding factors from 4 poles to 16 poles and from 6 slots to 24 slots.

TABLE I
WINDING FACTOR

Slot \ Pole	4	6	8	10	12	14	16
6	0.866		0.866	0.500		0.500	0.866
9	0.617	0.866	0.945	0.945	0.866	0.617	0.328
12			0.866	0.933		0.933	0.866
15			0.711	0.866		0.951	0.951
18				0.735	0.866	0.901	0.945
21						0.866	0.891
24						0.760	0.866

III. The Comparison of Design Parameters

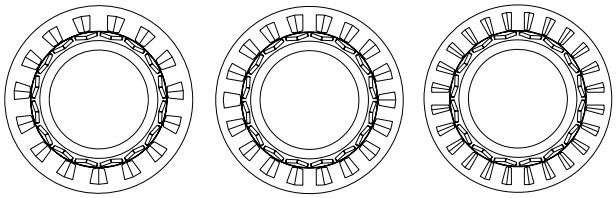

(a)16pole 15slots (b)16pole 18slots (c)16poles 24slots

Fig. 1. Three motor models.

In order to compare parameters of motor with different winding factors, three motor models are chosen and analyzed. In this paper three models are selected as shown in Fig.1. Fig.1 (a), (b) and (c) are 16poles 15slots, 16poles 18slots and 16poles 24slots models which are defined as model1, model2 and model3. Their winding factors are 0.866, 0.945 and 0.951 respectively. Finite Element Method (FEM) is used to calculate some parameters such as line-line BEMF, Total Harmonic Distortion (THD), cogging torque, saliency ratio. Having the same rotor structure, PM volume and fill-factor, the ratios of tooth width and yoke width in the three models are 1.86, 1.67 and 1.73 respectively.

A. Back EMF, THD, Cogging Torque

The Fig. 2 and Table II show line-line BEMF of model1, 2 and 3. Among three models, line-line BEMF of model1 is the largest and the most sinusoidal. Therefore THD of model1 is the lowest.

Cogging torque of three models is compared as shown in Fig. 3 and Table II. It is obvious that model1 has the lowest cogging torque. The line-line BEMF and cogging torque peak-peak value of model1 are chosen as the standard. And then values of the other two models are normalized.

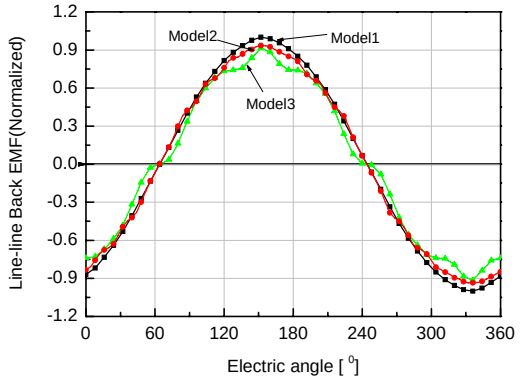

Fig. 2 The comparison of line-line Back EMF.

TABLE II
LINE-LINE BACK EMF, THD, COGGING TORQUE

Contents \ Model	Model1	Model2	Model3
Line-Line Back EMF(Normalized)	1	0.944	0.865
Winding Factor	0.951	0.945	0.866
THD(%)	0.71	3.28	9.2
Cogging Torque peak-peak(Normalized)	1	2.27	55.27

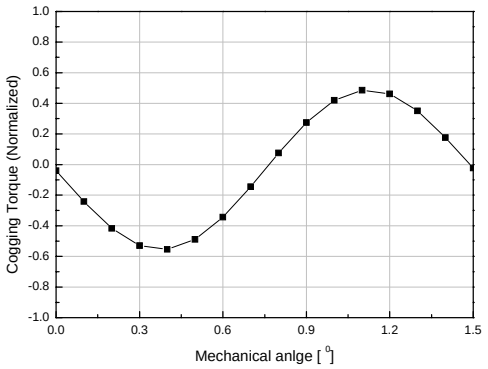

(a) model1

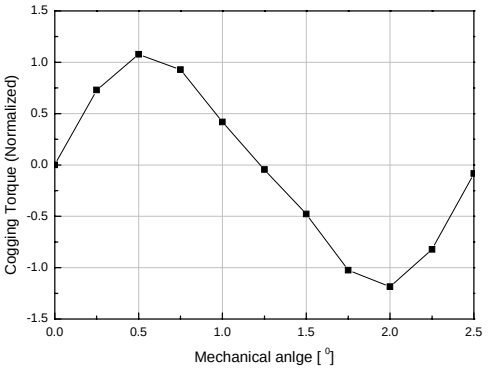

(b) model2

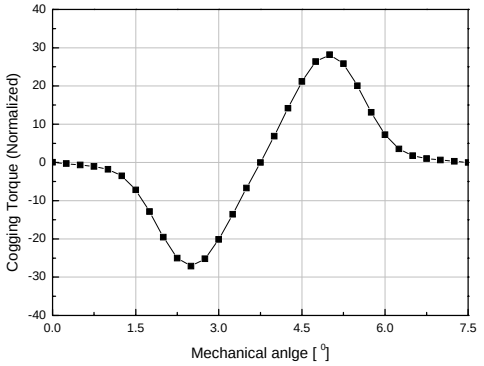

(c) model3

Fig. 3 Cogging torque of three models.

B. Torque and Torque ripple

Torque of IPMSM in normal operation is expressed in d-q coordinates as shown in equation (1). Torque of IPMSM is composed of magnetic torque and reluctance torque.

$$T = P_n\{\psi_a i_q + (L_d - L_q) i_d i_q\}$$
$$= P_n\{\psi_a i_a \cos\beta + \frac{1}{2}(L_q - L_d) I_a^2 \sin 2\beta\} \quad (1)$$

where P_n is pole pair number, $\psi_a = \sqrt{3/2}\psi_f$, ψ_f is peak armature flux linkage due to permanent magnets, i_d, i_q are d-q components of armature current, L_d, L_q are inductance along *d-q* axes, $I_a = \sqrt{3} I_e$, I_e is effective value of armature current, β is lead angle of current vector from q axis.

In order to compare torque and torque ripple of

model1, 2 and 3 with same current, the lead angle of current vector from q axis at the maximum torque must be checked. And the values of three models are 16°, 16° and 24°. Also the torque is calculated at $\beta = 0$ in order to confirm magnetic torque. The reluctance torque can be calculated by subtracting magnetic torque form maximum torque.

Fig. 4 and Table III show magnetic torque, reluctance torque, β at maximum torque, average torque and torque ripple. These parameters values of model1 are chosen as standard. And then values of the other two models are normalized. The results of average torque are same values but torque ripple and reluctance torque of model3 are largest. On the other hand, magnetic torque of model3 is lowest because Line-line BEMF of model3 is lowest.

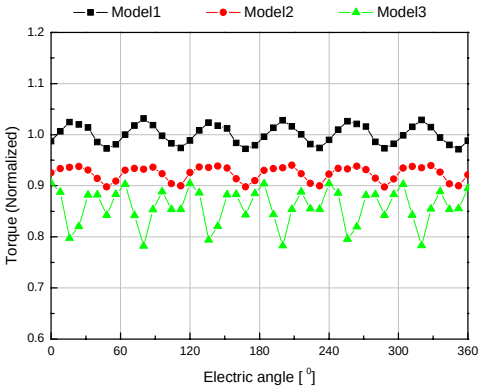

(a) Magnetic torque of three models.

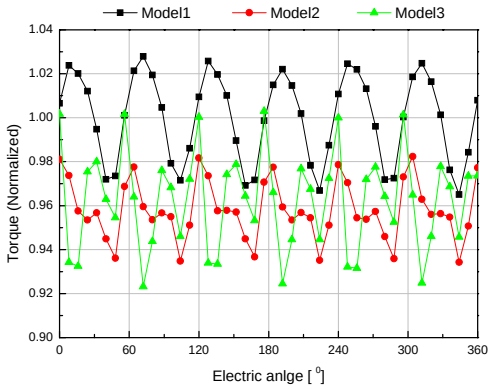

(b) Average torque of three models.

Fig. 4. Torque analysis.

TABLE III
THE RESULTS OF TORQUE

Contents \ Model	Model1	Model2	Model3
Magnetic Torque (Normalized)	1	0.924	0.860
Reluctance Torque (Normalized)	1	2.81	6.52
β at the maximum torque (°)	16	16	24
Average torque (Normalized)	1	0.958	0.963
Torque ripple (%)	6.3	5.02	8.3

C. D-q axes inductance and Saliency ratio

Since IPMSM has permanent magnet embedded in the rotor, it has a difference of d-q axes inductance. In case of saliency ratio which is defined as L_q/L_d is increased, reluctance torque will be increased. Fig. 5 (a), (b) and (c) show d-q axes inductance and saliency ratio of three models which are calculated from $\beta = 10^0$ to $\beta = 80^0$. The d axis inductance increases in order of model3, model2 and model1, and then the q axis inductance increases in order of model2, model3 and model1. Saliency ratio of Model3 is the largest due to the lowest d axis inductance. Therefore reluctance torque of model1 is the lowest as shown in Table III.

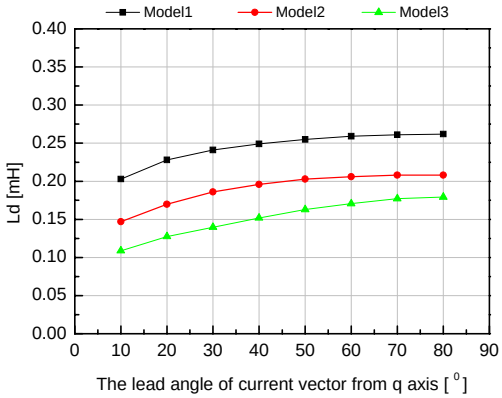

(a) Inductance of d axis.

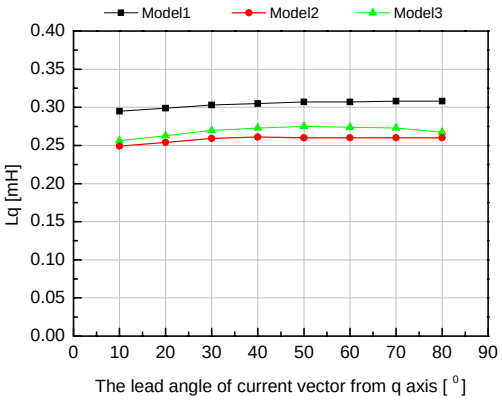

(b) Inductance of q axis.

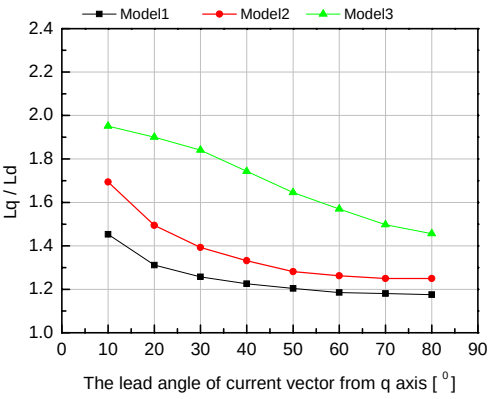

(c) Saliency ratio.

Fig. 5. D-q axes inductance and saliency ratio.

IV. Operating Performance

Voltage equation of IPMSM in normal operation is expressed in d-q coordinates as shown in equation (2).

$$\begin{bmatrix} v_d \\ v_q \end{bmatrix} = \begin{bmatrix} R_a + pL_d & -\omega L_q \\ \omega L_d & R_a + pL_q \end{bmatrix} \begin{bmatrix} i_d \\ i_q \end{bmatrix} + \begin{bmatrix} 0 \\ \omega \psi_a \end{bmatrix} \quad (2)$$

Where i_d, i_q are d-q components of armature current, v_d, v_q are d-q components of armature voltage, $\psi_a = \sqrt{3/2}\psi_f$, ψ_f is peak armature flux linkage due to permanent magnets, R_a is armature resistance, L_d, L_q are inductance along d-q axes, $p = d/dt$.

Various methods of current vector control have been proposed using the above d-q model. Since IPMSM is fed via inverter, the following limitations on armature current and terminal voltage must be considered.

$$I_a = \sqrt{i_d^2 + i_q^2} \le I_{am} \quad (3)$$

$$V_a = \sqrt{v_d^2 + v_q^2} \le V_{am} \quad (4)$$

Where I_{am} and V_{am} are ceiling values of current and voltage [1].

When maximum power control is executed, constant power operation region is determined by machine parameters, and pattern of speed-power characteristic is known to depend on $\psi_{d\min}$

$$\psi_{d\min} = \psi_a - L_d I_{am} \quad (5)$$

$\psi_{d\min}$ is the difference between flux linkage caused by permanent magnets, and maximum negative flux linkage caused by armature reaction along d-axis, which corresponds to minimum flux linkage along d-axis [3-4].

For $\psi_{d\min} > 0$, there is an output limit as follows.

$$\omega_c = \frac{V_{om}}{\psi_a - L_d I_{am}} = \frac{V_{om}}{\psi_{d\min}} \quad (6)$$

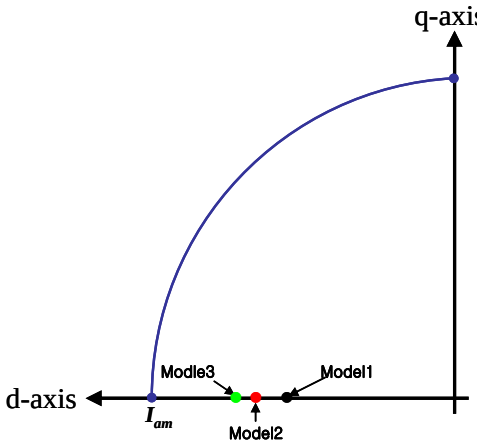

Fig. 6. Ψ_a/L_d of the three models.

The more $\psi_{d\min}$, the larger the maximum torque is, but at the same time, constant power operation region becomes narrow. On the other hand, $\psi_{d\min} \le 0$, there is no operating limit theoretically, and the less the absolute value of $\psi_{d\min}$, the larger is the output. Thus, $\psi_{d\min} = 0$ is the ideal condition to obtain very wide range of constant power [1].

As equation (5), ψ_a / L_d value is I_{am} in the case of $\psi_{d\min} = 0$. The ψ_a / L_d values of the three models are lower than I_{am} as shown in the Fig. 6. Therefore, three models are no operating limit at high-speed region. The $\psi_{d\min}$ value of model1 is the lowest because d axis inductance of Model1 is the lowest.

V. Conclusions

The results of design parameters of three models which have different winding factors show that design parameters, such as line-line BEMF, THD and cogging torque, of model3 are the best. However saliency ratio of model3 is the lowest.

The results of ψ_a / L_d values in the three models, which determines the constant torque region and the constant power region satisfy the power at the high-speed because the ψ_a / L_d value of these models is lower than I_{am}.

As mentioned above the results of design parameters and operating performance of model3 which has the largest winding factor are the best. Therefore choose of pole-slot combinations is important at initial design.

References

[1] Shigeo Morimoto, Yoji Takeda "Machine Parameters and Performance of Interior Permanent Magnet Synchronous Motors with Different Permanent Magnet Volume", *Electrical Engineering in Japan*, vol. 131, No. 4, 2000.

[2] Freddy Magnussen, Chandur Sadarangani, "Winding Factors and Joule Losses of Permanent Magnet Machines with Concentrated Windings", *Electric Machines and Drives Conference (IEMDC'03)*, Vol. 1, pp.333-339, June 2002.

[3] Takeda et al. *Control schemes for PM motors and comparative characteristics of various rotor designs.* Dengakuron; 114-D:662, 1994.

[4] Morimoto et al. *Wide-range variable-speed control of internal magnet motors.* Dengakuron; 114-D:668, 1994.

Welcome Message
Organizer & Committees
Sponsors
Sessions
Authors Index
Search

Welcome Message

Dear Colleagues,

It is a real pleasure and an honor for us to announce the 9th International Conference on Electrical Machines and Systems (ICEMS 2006) organized by the IEEJ Industry Applications Society (IAS).

ICEMS is the only major international conference devoted entirely to electrical machines and systems in Asia and provides an excellent opportunity for scientists and experts from all parts of the world to present recent developments and to exchange useful information and experiences from their research. In this conference, four outstanding professors are scheduled to offer presentations.

ICEMS 2006 concludes the first technical co-sponsorship with IEEE IAS. Each committee has been making every effort in the careful preparation of ICEMS 2006. We sincerely hope that ICEMS 2006 shall conclude successfully and ICEMS will go on to develop further as an important conference in this field.

On behalf of all the Committees of ICEMS 2006, I would like to say that we welcome you to the 9th International Conference on Electrical Machines and Systems (ICEMS 2006).

Sincerely,

Prof. Ichiro Miki
ICEMS 2006 Conference Chairman
October 23, 2006

DS2F1-06 PDF

A Study on the Improvement of Construction Error in Permanent Magnet Stepping Motor with Claw Pole

Dae Sung Jung, Seoun Bin Lim, Ju Lee
Hanyang University, Korea

DS2F1-07 PDF

Reduction of Torque Ripple Using Harmonic Current Injection in Interior Permanent Magnet Synchronous Motor

Ji-Hyung Bahn [1)], Sung-Il Kim [1)], Jung-Pyo Hong [1)], Geun-Ho Lee [2)]
[1)]Changwon Nat'l Univ, Korea, [2)]Gyeongnam Provincial Namhae Collage, Korea

DS2F1-08 PDF

The Acoustic Noise Reduction in Interior Permanent Magnet Motor by Structural and Electromagnetic Design

Sang-Ho Lee [1)], Suk-Hee Lee [1)], Jung-Pyo Hong [1)], Sang-Moon Hwang [2)]
[1)]Changwon National University, Korea, [2)]Pusan National University, Korea

DS2F1-09 PDF

A Sensorless Speed Control of IPMSM Using an Adaptive Integral Binary Observer

Hyoung Lee, Hyung Seok Kang, Young Seok Kim
Inha Univerrity, Korea

DS2F1-10 PDF

The Comparison of Characteristic and Operating Performance by Pole-Slot Combinations in Interior Permanent Magnet Synchronous Motor with Concentrated Winding

Seung-Hyoung Ha, Soon-O Kwon, Ji-Hyung Bahn, Jung-Pyo Hong
Chnagwon Nat'l. Univ, Korea

DS2F1-11 PDF

Optimum Design of Interior Permanent Magnet Synchronous Motor Using Taguchi Method

Ikuro Morita, Yuuki Hotta
University of Tokushima, Japan

DS2F1-12 PDF

Sensorless Drive for Brushless DC Motor Using Simple Voltage Detecting Circuit

Sung-Chul Go [1)], Seung-Joo Kim [1)], Sol Kim [2)], Seung-Bin Lim [1)], Joon-Seon Ahn [1)], Seung-Kil Choi [3)], Ju Lee [1)]
[1)]Hanyang University, Korea, [2)]Yuhan College, Korea, [3)]Ansan College, Korea

DS2F1-13 PDF

Torque Ripple Reduction of Multi-Layer Design Interior Permanent Magnet Motor Using Response Surface Methodology

Liang Fang, Soon-O Kwon, Peng Zhang, Jung-Pyo Hong
Changwon National University, Korea

DS2F1-14 PDF

Prediction of Efficiency and Torque Characteristic on Concentrated Winding IPMSM with Wide Speed Range

Sung-Il Kim [1)], Ji-Hyung Bhan [1)], Jung-Pyo Hong [1)], Ki-Chae Lim [2)]
[1)]Changwon National University, Korea, [2)]Dongsung Electric Machine Co. Ltd, Korea

DS2F1-15 PDF

Improvement of Ozone Yielding Characteristic Using a DSP Controlled Multilevel Resonant Inverter

Sung-Geun Song [1)], Feel-Soon Kang [2)], Sung-Jun Park [1)], Yu Tao [1)], Chae-Joo Moon [3)]
[1)]Chonnam National University, Korea, [2)]Hanbat National University, Korea, [3)]Mokpo National University, Korea